Acta Crystallographica Section D
Biological Crystallography
ISSN 0907-4449

Structure of an RNase-related protein from *Calystegia sepium*

A. Rabijns,[a] C. Verboven,[a] P. Rougé,[b] A. Barre,[b] E. J. M. Van Damme,[c] W. J. Peumans[c] and C. J. De Ranter[a]*

[a]Laboratory of Analytical Chemistry and Medicinal Physicochemistry, Faculty of Pharmaceutical Sciences, K. U. Leuven, E. Van Evenstraat 4, B-3000 Leuven, Belgium, [b]Institut de Pharmacologie et Biologie Structurale, UMR-CNRS 5089, 205 Route de Narbonne, 31077 Toulouse CEDEX 4, France, and [c]Laboratory for Phytopathology and Plant Protection, Faculty of Agricultural and Applied Biological Sciences, K. U. Leuven, W. de Croylaan 42, B-3001 Leuven, Belgium

Correspondence e-mail: camiel.deranter@farm.kuleuven.ac.be

Received 15 October 2001
Accepted 7 February 2002

PDB Reference: CalsepRRP, 1jy5, r1jy5sf.

The structure of a catalytically inactive RNase-related protein from *Calystegia sepium* (CalsepRRP) has been resolved by protein crystallography at a resolution of 2.05 Å and an *R* factor of 20.74%. Although the protein is completely devoid of ribonuclease activity, it adopts the typical $\alpha + \beta$ structure of non-base-specific RNases. Analysis of the structure revealed that two amino-acid substitutions in the 'active' P1 site, in combination with the less hydrophobic/aromatic character of the B1 base-recognition site and a completely disrupted B2 base-recognition site, might account for this complete lack of activity.

1. Introduction

Ribonucleases (RNases; EC 3.1.27) are an extended group of enzymes that are capable of cleaving RNA by catalyzing the hydrolysis of the 3′:5′-phosphodiester bond between two adjacent nucleotides. According to their molecular mass and base specificity, RNases are classified into three distinct groups. Pyrimidine base-specific RNases with a molecular mass of approximately 14 kDa constitute a first group, whereas a second group consists of 12 kDa guanosine-specific RNases. A third group comprises non-base-specific RNases with molecular masses around 24–30 kDa. Classical examples of the latter group are RNase T_2 from *Aspergillus oryzae*, RNase Rh from *Rhizopus niveus* and the typical plant RNase LE from *Lycopersicon esculentum* (tomato).

RNases have been studied intensively in flowering plants. At present, the superfamily of plant RNases is subdivided in S-RNases and S-like RNases (Green, 1994; Richman *et al.*, 1997). The S-RNases are present in high concentrations in the transmitting tract of the styles of self-incompatible Rosaceae, Solanaceae and Scrophulariaceae species and are believed to play an important role in gametophytic self-incompatibility (Green, 1994; Royo *et al.*, 1994). S-like RNases (also called non-S-RNases) have been identified in various tissues of numerous monocots and dicots. Unlike the basic S-RNases, all S-like RNases (except the seed RNases from the Cucurbitaceae species *Momordica charantia* and *Luffa cylindrica*) have an acidic isoelectric point.

During the last few years, evidence has been presented for the occurrence of proteins that closely resemble typical plant RNases but are devoid of catalytic activity. A self-compatible accession of *Lycopersicon peruvianum* contains a stylar S-RNase that has lost its catalytic activity owing to the substitution of a histidine residue by an asparagine in the active site (Royo *et al.*, 1994). More recently, the major storage protein from rhizomes of hedge bindweed (*Calystegia sepium*) has been identified as a protein that closely resembles RNases

from the T_2 family with respect to its amino-acid sequence but lacks RNase activity, presumably because of the replacement of a single catalytically important histidine residue by a lysine (Van Damme *et al.*, 2000). As the so-called *C. sepium* RNase-related protein (CalsepRRP) is an abundant protein, it offered a unique opportunity for a structural study of an enzymatically inactive S-like RNase homologue and to corroborate the structural differences between active and inactive sites at the atomic level.

Here, we report the crystal structure of CalsepRRP at 2.05 Å resolution as determined by molecular replacement. This is the first structure of a vegetative storage protein from plants that is closely related to the RNase T_2 family. Structural comparison of CalsepRRP with fungal as well as plant RNases indicates that the overall fold of the RNase structure is conserved; specific features in the 'active' P1 site and the B1 and B2 base-recognition sites are postulated to account for the inactivity of CalsepRRP.

2. Materials and methods

2.1. Purification and crystallization

A total preparation of CalsepRRP was isolated from rhizomes of *C. sepium* by classical protein-purification techniques and separated into its constituent glycosylated and unglycosylated isoforms by affinity chromatography on immobilized concanavalin A (Van Damme *et al.*, 2000). Only the purified unglycosylated form was used for the crystallization experiments. Crystals suitable for diffraction analysis (Fig. 1) were grown at 277 K using the hanging-drop vapour-diffusion technique from a solution containing 0.2 *M* NaCl, 0.1 *M* acetate buffer pH 4.6, 30% MPD and 10 mg ml^{-1} CalsepRRP.

2.2. Data collection

Data collection with cryocooling at 100 K was carried out at the X11 beamline of the DESY synchrotron (Hamburg, Germany). The crystals, with typical dimensions of 0.3 × 0.3 × 0.3 mm, diffracted to 2.05 Å and the space group was assigned to be $P6_2$ or $P6_4$, with unit-cell parameters a = 121.69, b = 121.69, c = 66.059 Å. Data processing was performed using *DENZO* and *SCALEPACK* (Otwinowski & Minor, 1997).

Figure 1
Crystals of CalsepRRP with typical dimensions of 0.3 × 0.3× 0.3 mm.

Table 1
Crystallographic data for the CalsepRRP structure.

Values in parentheses are for the highest resolution shell.

Data collection	
Space group	$P6_2$
Wavelength (Å)	0.9116
Beamline	X11, DESY Hamburg
Unit-cell parameters (Å, °)	a = 121.69, b = 121.69, c = 66.06, α = 90, β = 90, γ = 120
Resolution limits (Å)	30–2.05 (2.09–2.05)
Total observations	163993 (7023)
Unique reflections	35416 (1739)
Completeness (%)	99.8 (100.0)
Completeness ($I > 2\sigma$) (%)	85.5 (66.3)
$\langle I/\sigma(I)\rangle$	20.71 (5.12)
R_{sym} (%)	6.3 (33.8)
Refinement	
R_{work} (%)	20.74
R_{free} (%)	24.20
No. of atoms in protein/solvent	3146/375
Mean B in protein/solvent (Å^2)	28.34/31.21
R.m.s.d. bond lengths (Å)	0.005
R.m.s.d. bond angles (°)	1.230
R.m.s.d. B, bonded main chain (Å^2)	1.443
R.m.s.d. B, bonded side chain (Å^2)	2.039

The calculated Matthews coefficient (Matthews, 1974) of 2.56 Å^3 Da^{-1} suggests that the asymmetric unit consists of two molecules. This twofold non-crystallographic symmetry (NCS) was also confirmed in a self-rotation search. The data-collection statistics for the data set are summarized in Table 1.

2.3. Determination and refinement of the structure

The phase problem was solved with the molecular-replacement technique in *AMoRe* (Navaza, 1994) using the coordinates of the extracellular ribonuclease from *L. esculentum* RNase LE (PDB code 1dix; Tanaka *et al.*, 2000) as a search model. Using space group $P6_2$, two peaks were found in the translation search corresponding to the two molecules in the asymmetric unit. The R factor after initial rigid-body refinement to 3 Å was 52.4%. All attempts to solve the crystallographic phase problem by molecular replacement using the structures of other RNases, *e.g.* from *R. niveus* RNase Rh (Kurihara *et al.*, 1996) and *M. charantia* RNase MC1 (Nakagawa *et al.*, 1999), were unsuccessful.

Refinement of the CalsepRRP structure was performed in the *CNS* package (Brünger *et al.*, 1998) using torsional angle dynamics and individual B-factor refinement. A randomly selected 10% of the data set was set aside for cross-validation using the R_{free} value and bulk-solvent correction was used. In the initial stages of refinement, strict NCS restraints were used between the two molecules in the asymmetric unit. However, it soon became clear that imposing NCS restraints substantially hindered the refinement of certain loops and resulted in high B values and poor electron-density maps. The reason for this is that in both molecules some loop regions do not have the same structural features. Therefore, the NCS restraints were dropped in the later stages of refinement. During refinement, solvent molecules were progressively added when they met the following requirements: (i) a minimum 3σ peak had to be present in the $|F_{obs}| - |F_{calc}|$ difference map, (ii) a

Table 2
Crystallographic R factor and R_{free} as a function of resolution (based on F/σ cutoff = 0).

	R	R_{free}
500.0–4.42	0.2034	0.2283
4.42–3.51	0.1769	0.2148
3.51–3.06	0.2126	0.2273
3.06–2.78	0.2213	0.2704
2.78–2.58	0.2183	0.2799
2.58–2.43	0.2110	0.2285
2.43–2.31	0.2234	0.2619
2.31–2.21	0.2192	0.2421
2.21–2.12	0.2143	0.2482
2.12–2.05	0.2280	0.2941

peak had to be visible in the $2|F_{obs}| - |F_{calc}|$ map, (iii) the B value for the water molecule should not exceed 60 Å^2 during refinement and (iv) the water molecule had to be stabilized by hydrogen bonding. Visual inspection and model building were performed using the program *O* (Jones *et al.*, 1991). Assessment of the quality of the coordinates was performed with the programs *PROCHECK* (Laskowski *et al.*, 1993) and *MOLEMAN* (Kleywegt & Jones, 1997). Molecular graphics were generated with *MOLSCRIPT* (Kraulis, 1991), *BOBSCRIPT* (Esnouf, 1997) and *Raster3D* (Merritt & Bacon, 1997). The coordinates were deposited in the Protein Data Bank (Bernstein *et al.*, 1977).

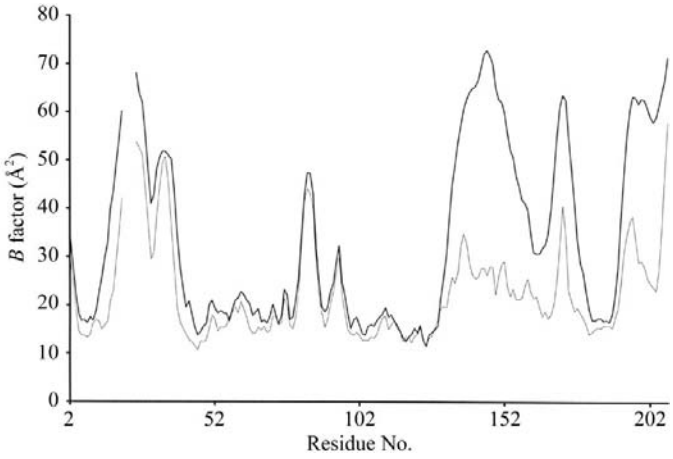

Figure 2
Graphical representation of B factors for the A molecule (thin line) and B molecule (thick line) as a function of the residue number.

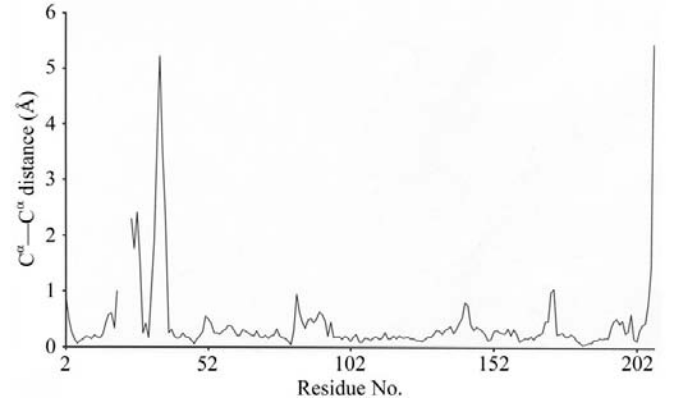

Figure 3
$C^{\alpha}-C^{\alpha}$ distance (Å) between corresponding atoms of the A and B molecule of CalsepRRP.

3. Results and discussion

3.1. Quality of the structure of CalsepRRP

The final model of CalsepRRP converged to an R factor of 20.74% and an R_{free} value of 24.20% (Table 1). It comprises two CalsepRRP molecules A and B (each with 203 amino-acid residues out of a total of 212 residues) and 375 water molecules. The first N-terminal and the four C-terminal residues (209–212) are disordered.

The model has a good geometry and shows r.m.s. deviations from ideal bond lengths and angles of 0.005 Å and 1.230°, respectively. 86.8% of the residues are found in the most favoured regions of the Ramachandran plot and 12.9% in the additional allowed regions. One of the residues (residue 172 in molecule A) was consistently found in the disallowed regions. However, electron density in this region clearly showed that this residue is correctly positioned and all attempts to place this residue in the allowed regions were unsuccessful. Further

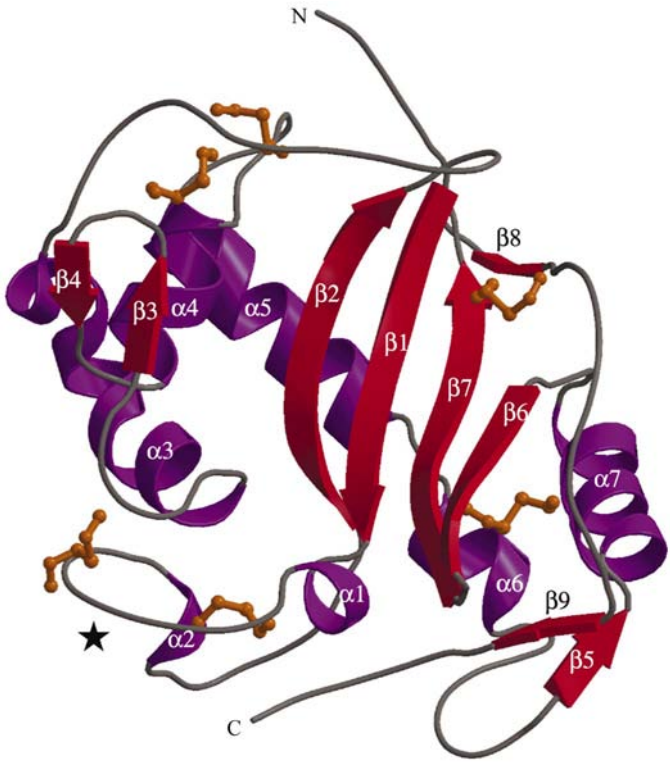

Figure 4
Ribbon diagram of the three-dimensional structure of CalsepRRP. β-sheet strands (numbered $\beta1$–$\beta9$) are indicated by red arrows and α-helices (numbered $\alpha1$–$\alpha7$) are coloured violet. The missing part of the loop connecting helices $\alpha1$ and $\alpha2$ of CalsepRRP is indicated by a line marked by a star. The six disulfide bridges Cys19–Cys31, Cys26–Cys84, Cys57–Cys90, Cys58–Cys108, Cys170–Cys198 and Cys181–Cys191 are coloured orange.

refinement statistics are given in Table 1 and the crystallographic R factor as a function of resolution is tabulated in Table 2. The average temperature factors for the main-chain and side-chain atoms are 28.07 and 28.62 Å^2, respectively, but a significant difference is observed between the average temperature factor for molecule A (23.10 Å^2 for all atoms) and molecule B (33.58 Å^2 for all atoms). This difference between the molecules is mainly caused by higher B factors in the C-terminal half of the B molecule (residues 131–203; Fig. 2). As can be judged from packing analysis, the region consisting of residues 131–203 is stabilized by crystal contacts in the A molecule; the corresponding region in the B molecule lacks such stabilizing crystal contacts, causing higher flexibility. Furthermore, a plot depicting the B factors of the main-chain atoms for both molecules A and B shows that in the two molecules one loop region (19–30) has very high B factors (Fig. 2). Owing to this disorder, residues 21–24 could not be unambiguously built in the electron-density map. On superposing molecules A and B it can be seen that both molecules are very similar except for the differences in the aforementioned flexible loop. A plot of the distance between corresponding C$^\alpha$ atoms of the A and B molecule is shown in Fig. 3. The total r.m.s. deviation for all C$^\alpha$ atoms is 0.61 Å. The mean temperature factor of the 375 water molecules is 31.21 Å^2.

3.2. Structure description

As shown in the ribbon diagram of the A molecule of CalsepRRP (Fig. 4), the protein adopts an $\alpha + \beta$ structure similar to that of RNases from plants and fungi, with approximate dimensions of 50 × 40 × 25 Å. The three-dimensional fold closely resembles that of RNase Rh from the fungus *R. niveus* (Kurihara *et al.*, 1996) and the plant RNases from *L. esculentum* RNase LE (Tanaka *et al.*, 2000) and *M. charantia* RNase MC1 (Nakagawa *et al.*, 1999) (Fig. 5), with C$^\alpha$ r.m.s. deviations of 1.38, 1.13 and 1.54 Å, respectively, for the residues in the conserved secondary-structure elements. Despite a few discrepancies, which mainly concern the insertion or deletion of more-or-less extended loops and the number and location of the disulfide bridges, all these proteins share a similar organization of the β-sheet strands and α-helices. According to the hydrogen-bonding pattern between the main-chain atoms and the values of the φ and ψ dihedral angles of the peptide bonds, seven α-helices and nine β-strands can be identified in the CalsepRRP structure (Figs. 4 and 6). The α-helices are α1 (15–19), α2 (30–33), α3 (64–79), α4 (96–105), α5 (115–130), α6 (131–138) and α7 (151–163). The five β-strands β1 (7–14), β2 (40–48), β6 (167–171), β7 (174–182) and β8 (188–189) form sheet A, whereas the two strands β5 (149–150) and β9 (201–202) form sheet B, and strands β3 (87–89) and β4 (92–94) form sheet C. Interestingly, the loop connecting helices α3 and α4 in CalsepRRP is considerably longer than the corresponding loop in RNase LE, RNase Rh and RNase MC1. Moreover, this long loop, which folds back over the structure, forms a β-sheet composed of strands β3 and β4 and is stabilized by a unique disulfide bridge between Cys57 and Cys90. In this respect, CalsepRRP (with six disulfide bridges) clearly differs from RNase Rh (with five disulfide bridges), RNase LE (with five disulfide bridges) and RNase MC1 (with

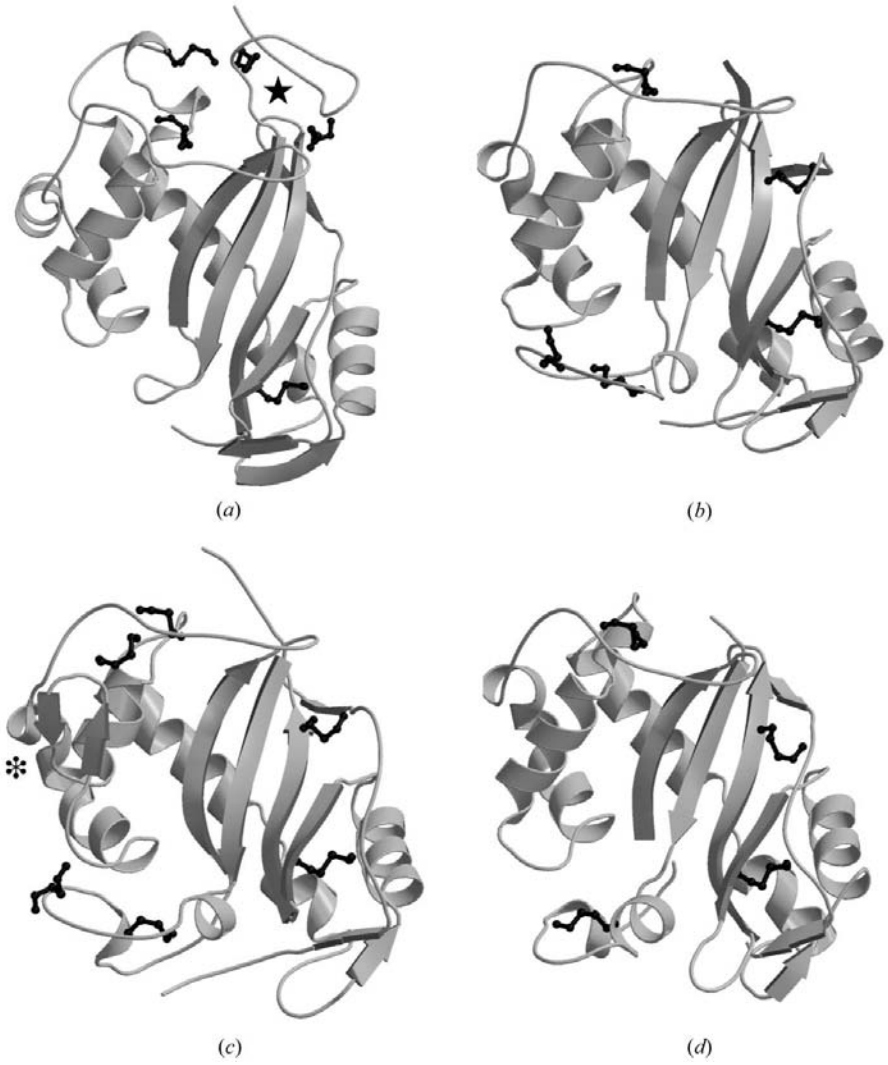

Figure 5
Overall three-dimensional structures of RNase Rh (*a*), RNase MC1 (*b*), CalsepRRP (*c*) and RNase LE (*d*). β-sheet strands are indicated by arrows. Cysteine residues involved in disulfide bonds are in ball-and-stick and coloured black. The N-terminal extra-loop sequence of RNase Rh is indicated by a star. The modelled part of the loop connecting helices α1 and α2 of CalsepRRP is indicated by an asterisk.

four disulfide bridges). It is also worth noting that only two pairs of Cys residues are common to all these RNases (namely Cys58–Cys108 and Cys170–Cys198). A description of all the disulfide bridges is presented in Table 3.

Like RNase LE (IEP 4.89) and RNase Rh (IEP 4.80), CalsepRRP exhibits a rather acidic surface, which is in good agreement with the calculated isoelectric point of 4.87.

Analysis of the electron density of the CalsepRRP structure unambiguously demonstrated the occurrence of a single *cis*-peptide bond between Ser110 and Pro111. No such *cis*-peptide bond can be found in the corresponding regions of RNase LE, RNase Rh and RNase MC1.

3.3. The P1 site

The 2′:3′-cyclizing RNases, which cleave phosphodiester bonds of RNA to release 2′:3′-cyclic nucleotides that yield 3′-nucleotides upon subsequent hydrolysis, are classified into three distinct groups on the basis of their molecular masses and amino-acid sequences. CalsepRRP is structurally related to the group of high molecular-weight (24 kDa) RNases, which also includes RNase T_2 (*A. oryzae*), RNase M (*A. saitori*), RNase Rh (*R. niveus*) as well as RNase MC1 from the bitter gourd (*M. charantia*), RNase LE from tomato (*L. esculentum*) and all plant S-RNases (Parry *et al.*, 1998; Ishimizu *et al.*, 1998). Chemical modification and site-directed mutagenesis experiments (Sanda, Takizawa & Irie, 1985; Sanda, Takizawa, Iwama *et al.*, 1985; Ohgi *et al.*, 1993) indicated that two histidine residues (His46 and His109) and a single carboxylic residue (Glu105) form the catalytic site (the so-called P1 site) of RNase Rh. These residues, which are located in the centre of a deep cleft, interact with each other either directly (Glu105 $O^{\varepsilon1}$—His46 $N^{\varepsilon2}$, 3.20 Å) or indirectly *via* a bridging water molecule (Glu105 $O^{\varepsilon2}$—Wat, 2.67 Å; His104 $N^{\varepsilon2}$—Wat, 2.78 Å; His109 $N^{\varepsilon2}$—Wat, 2.91 Å). Most probably, two other basic residues (His104 and Lys108) also participate in the binding of the substrate. Structural studies and molecular modelling (Kurihara *et al.*, 1996) further suggested that the active site is surrounded by a hydrophobic pocket (containing Trp49), which contributes to the RNase activity because the aromatic residue preserves the active-site conformation through a hydrogen bond with the side chain of Glu105 (Glu105 $O^{\varepsilon1}$—Trp49 $N^{\varepsilon2}$, 2.93 Å). Plant RNases possess similarly oriented basic and acidic residues. His39, His92, Glu93, Lys96 and His97 of RNase LE, and His34, His83, Glu84, Lys87 and His88 of RNase MC1 correspond to His46, His104, Glu105, Lys108 and His109 of RNase Rh, respectively. Both RNases also possess a Trp residue (Trp42 of RNase LE and Trp37 of RNase MC1) homologous to Trp49 of RNase Rh and form similar hydrogen bonds to the Glu (Glu93 of RNase LE and Glu84 of RNase MC1) residue. However, owing to a rather distinct location of water molecules inside the P1 sites of the different RNases, some discrepancies occur in the network of hydrogen bonds interconnecting the residues and water molecules (Fig. 7).

Residues Glu101, Lys104 and His105 of CalsepRRP, which are homologous to Glu105, Lys108 and His109 of RNase Rh, respectively, are similarly oriented in the three-dimensional structure, whereas residue Lys43, which is homologous to His46 of RNase Rh, is shifted away more than 4.50 Å from Glu101. Tyr100 (homologous to His104 of RNase Rh) interacts with Lys104 through a weak hydrogen bond. The aromatic residue Trp46 is similarly oriented to Trp49 of RNase Rh and hence is in principle capable of preserving the conformation of the active site in CalsepRRP (Fig. 7). However, owing to the replacement of two amino-acid residues, the discrete conformation of the active site considerably differs from that of RNase Rh and the different plant RNases. Residues Lys43 (homologous to His46 of RNase Rh) and His105 (homologous to His109 of RNase Rh) of CalsepRRP are separated from each other by 8.39 Å. This distance is considerably increased

Table 3
Disulfide-bridge pattern in CalsepRRP and other RNases.

CalsepRRP	RNase LE	RNase MC1	RNase Rh
19–31	18–24	15–23	—
26–84	25–81	—	—
57–90	—	—	—
58–108	54–100	48–91	63–112
170–198	161–196	151–184	182–213
181–191	177–188	168–179	—
—	—	—	3–20
—	—	—	10–53
—	—	—	19–120

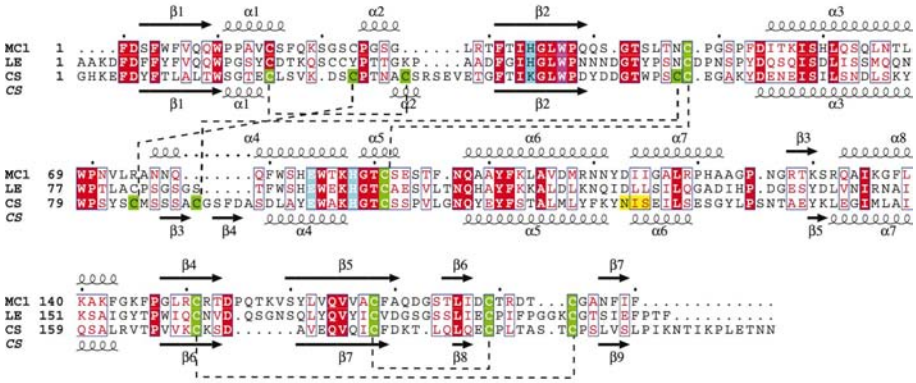

Figure 6
Sequence alignment of RNase MC1 (MC1), RNase LE (LE) and CalsepRRP (CS) performed with *ESPript* (Gouet *et al.*, 1999). Multiple sequence alignment was performed with *ClustalW* (Thompson *et al.*, 1994) and modified according to the structural homologies inferred from the superposition of the crystallographic structures. Invariant (red boxes) and conserved (blue boxes) residues are indicated. Conserved Cys residues are in green and dashed grey lines indicate the disulfide bridges of CalsepRRP. Invariant residues involved in the P1 site are coloured cyan (His and Glu) and magenta (Trp). The putative *N*-glycosylation site is shown in yellow. Secondary-structure elements of RNase MC1 and CalsepRRP are indicated above and below the sequences, respectively. β-sheet strands(β1–9) and α-helices (α1–8) are numbered.

compared with that in RNase LE (7.01 Å between His39 $N^{\varepsilon 2}$ and His97 $N^{\varepsilon 2}$), RNase MC1 (6.30 Å between His34 $N^{\varepsilon 2}$ and His88 $N^{\varepsilon 2}$) and RNase Rh (6.71 Å between His46 $N^{\varepsilon 2}$ and His109 $N^{\varepsilon 2}$) and this could prevent the basic residues fulfilling their catalytic role. In addition, the replacement of His104 of RNase Rh (His83 of RNase MC1, His92 of RNase LE) by Tyr100 in CalsepRRP eliminates a positive charge which is required to interact with the negatively charged phosphate group of the substrate. These two amino-acid changes presumably account for the inactivity of the *C. sepium* RNase-like protein CalsepRRP.

3.4. The putative B1 site and B2 site

The so-called B1 site (base-recognition site for the base at the 5′ side of the scissile phosphodiester bond) of RNases (Richards & Wyckoff, 1971), which is responsible for the accommodation of a purine base (adenine or guanine) of the substrate RNA, consists of a hydrophobic pocket located in the vicinity of the P1 site and is comprised of aromatic residues (Tyr8, Trp42, Tyr50 and Tyr175 of RNase LE; Tanaka *et al.*, 2000). The corresponding pocket of CalsepRRP comprises residues Thr9, Trp46, Trp54 and Gln179. As a result, this pocket is far less hydrophobic/aromatic, which severely hampers the stacking required for the binding of the purine bases. This phenomenon also may contribute to the lack of activity of CalsepRRP. Compared with the active RNases, very little conservation occurs in the so-called B2 site (the base-recognition site for the base at the 3′ side of the scissile bond; Richards & Wyckoff, 1971) of CalsepRRP. Interestingly, this B2 site in CalsepRRP coincides with an insertion of a few extra residues containing a Cys residue (Cys90) involved in a specific disulfide bond which has no equivalent in other plant or fungal RNases.

4. Discussion

Previous work revealed that the most abundant protein in rhizomes of *C. sepium* (hedge bindweed) shares a high sequence identity and similarity with non-base-specific RNases but is devoid of enzymatic activity (Van Damme *et al.*, 2000). Although sequence comparisons suggested that the lack of RNase activity of CalsepRRP could be attributed to the replacement of a single histidine residue by a lysine residue, conclusive evidence for the detrimental effect of this substitution is still missing. Since CalsepRRP can readily be isolated in reasonable amounts, this protein offered a unique opportunity to corroborate at the atomic level the impact of amino-acid residue substitutions on the activity of a natural mutant of a plant RNase.

The present structure of CalsepRRP at 2.05 Å resolution demonstrates that in spite of its complete lack of activity CalsepRRP adopts the same overall $\alpha + \beta$ structure as the active non-base-specific RNases from *L. esculentum* (Tanaka *et al.*, 2000) and *M. charantia* (Nakagawa *et al.*, 1999). Apart from a few differences, which are mainly restricted to the insertion or deletion of a few residues in loops and the number and location of disulfide bridges, all these proteins share a similar organization of the β-sheet strands and α-helices. As a result, the catalytic site P1 exhibits a high degree of both conformational and chemical conservation even though the water molecules associated with the site occupy different positions. However, a careful analysis of the data revealed that two amino-acid substitutions (namely His→Lys43 and His→Tyr100) in the 'active' site of CalsepRRP, in combination with the less hydrophobic/aromatic character of the B1 site and a completely disrupted B2 site, might be the elicitors of the complete lack of activity of this natural RNase mutant. Site-directed mutagenesis experiments should provide some support for this proposal. The present results reveal for the first time arguments in favour of the thesis that plants succeeded in generating a physiologically inactive homologue using a catalytically active RNase as a template by the replacement of a few amino-acid residues. As has been demonstrated previously, CalsepRRP behaves as a typical vegetative-storage protein (Van Damme *et al.*, 2000). This implies that somewhere during evolution an ancestor of *C. sepium* used an RNase gene as a template for a gene encoding a biologically inactive storage protein. Similar evolutionary events whereby duplicate copies of genes encoding enzymes or other biologically active proteins acquired a promoter that directs abundant expression

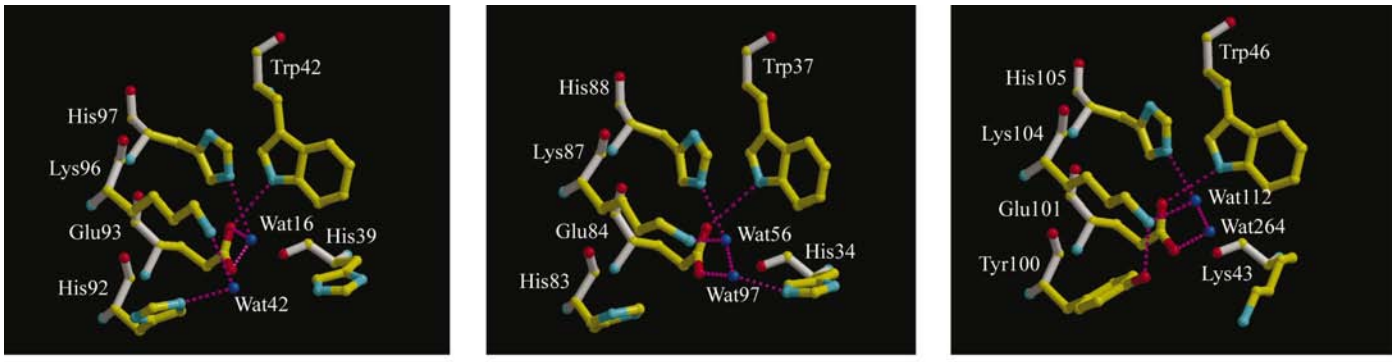

Figure 7
Residues forming the P1 site of RNase LE (*a*), RNase MC1 (*b*) and CalsepRRP (*c*). The water molecules (wat) correspond to blue spheres and magenta dashed lines indicate the networks of hydrogen bonds.

according to the storage needs of a specific organ have been documented in several plant species from different taxonomic groups (Staswick, 1994). In general, vegetative-storage proteins exhibit a high stability against denaturing agents and proteolytic enzymes. This also applies to CalsepRRP as this protein shares its overall structure with RNases, which are renowned for their extreme stability. Possibly, the extra disulfide bridge sustaining the three-dimensional fold of CalsepRRP renders this protein even more resistant than the active RNases and accordingly provides the plant with a highly resistant vegetative-storage protein.

AR is a Postdoctoral Research Fellow of the Fund for Scientific Research-Flanders (Belgium) and CV is a Postdoctoral Research Fellow of the K. U. Leuven Research Fund (OT/98/38). The financial support of CNRS is gratefully acknowledged (PR, AB). We thank the beamline scientists at DESY for technical support and the European Union for support of the work at EMBL Hamburg through the HCMP to Large Installations Project, contract No. CHGE-CT93-0040.

References

Bernstein, F. C., Koetzle, T. F., Williams, G. J. B., Meyer, E. F. Jr, Brice, M. D., Rodgers, J. R., Kennard, O., Shimanouchi, T. & Tasumi, M. (1977). *J. Mol. Biol.* **112**, 535–542.

Brünger, A. T., Adams, P. D., Clore, G. M., Delano, W. L., Gros, P., Grosse-Kunstleve, R. W., Jiang, J. S., Kuszewski, J., Nilges, M., Pannu, N. S., Read, R. J., Rice, L. M., Simonson, T. & Warren, G. L. (1998). *Acta Cryst.* D**54**, 905–921.

Esnouf, R. M. (1997). *J. Mol. Graph.* **15**, 132–134.

Gouet, P., Courcelle, E., Stuart, D. I. & Metoz, F. (1999). *Bioinformatics*, **15**, 305–308.

Green, P. J. (1994). *Annu. Rev. Plant Physiol. Mol. Biol.* **45**, 421–445.

Ishimizu, T., Endo, T., Yamaguchi-Kabata, Y., Nakamura, K. T., Sakiyama, F. & Norioka, S. (1998). *FEBS Lett.* **440**, 337–342.

Jones, T. A., Zhou, J. Y., Cowtan, S. & Kjeldgaard, M. (1991). *Acta Cryst.* A**47**, 110–119.

Kleywegt, G. J. & Jones, T. A. (1997). *Methods Enzymol.* **277**, 208–230.

Kraulis, P. J. (1991). *J. Appl. Cryst.* **24**, 946–950.

Kurihara, H., Nonaka, T., Mitsui, Y., Ohgi, K., Irie, M. & Nakamura, K. T. (1996). *J. Mol. Biol.* **255**, 310–320.

Laskowski, R. A., MacArthur, M. W., Moss, D. S. & Thornton, J. M. (1993). *J. Appl. Cryst.* **26**, 283–291.

Matthews, B. W. (1974). *J. Mol. Biol.* **82**, 513–526.

Merritt, E. A. & Bacon, D. J. (1997). *Methods Enzymol.* **277**, 505–524.

Nakagawa, A., Tanaka, I., Sakai, R., Nakashima, T., Funatsu, G. & Kimura, M. (1999). *Biochim. Biophys. Acta*, **1433**, 253–260.

Navaza, J. (1994). *Acta Cryst.* A**50**, 157–163.

Ohgi, K., Horiuchi, H., Watanabe, H., Iwama, M., Takagi, M. & Irie, M. (1993). *J. Biochem.* **113**, 219–224.

Otwinowski, Z. & Minor, W. (1997). *Methods Enzymol.* **276**, 307–326.

Parry, S., Newbigin, E., Craik, D., Nakamura, K. T., Bacic, A. & Oxley, D. (1998). *Plant Physiol.* **116**, 463–469.

Richards, F. & Wyckoff, H. W. (1971). *The Enzymes*, edited by P. D. Boyer, pp. 647–806. New York: Academic Press.

Richman, A. D., Broothaerts, W. & Kohn, J. R. (1997). *Am. J. Bot.* **84**, 912–917.

Royo, J., Kunz, C., Kowyama, Y., Anderson, M., Clarke, A. E. & Newbigin, E. (1994). *Proc. Natl Acad. Sci. USA*, **91**, 6511–6514.

Sanda, A., Takizawa, Y. & Irie, M. (1985). *Chem. Pharm. Bull.* **33**, 4515–4521.

Sanda, A., Takizawa, Y., Iwama, M. & Irie, M. (1985). *J. Biochem.* **98**, 125–132.

Staswick, P. E. (1994). *Annu. Rev. Plant Physiol. Mol. Biol.* **45**, 303–322.

Tanaka, N., Arai, J., Inokuchi, N., Koyama, T., Ohgi, K., Irie, M. & Nakamura, K. T. (2000). *J. Mol. Biol.* **298**, 859–873.

Thompson, J. D., Higgins, D. G. & Gibson, T. J. (1994). *Nucleic Acids Res.* **22**, 4673–4680.

Van Damme, E. J. M., Hao, Q., Barre, A., Rouge, P., Van Leuven, F. & Peumans, W. J. (2000). *Plant Physiol.* **122**, 433–445.